Efficient Long-Distance Entanglement with Quantum Repeaters under Decoherence and Purification

Wenhan Li
wenhanli@umass.edu

Shiyu Zhang
shiyuzhang@umass.edu

Abstract

We simulate a quantum network aimed at efficiently entangling two distant parties—Alice and Bob—via quantum repeaters using the Barrett-Kok (BK) scheme. The simulation models continuous-time depolarization as the dominant noise source and incorporates the BBPSSW purification protocol to restore entanglement fidelity. Our approach evaluates the trade-offs between generation time, fidelity, and resource cost, offering insights into optimizing entanglement distribution over long distances. Code and implementation details are available at: https://github.com/OceanCatSZ/cs690qc_final*. All of the modeling assumptions reference information from class slides.*

1. Introduction

Entanglement is fundamental to quantum communication, yet generating high-fidelity entanglement between distant parties (e.g., Alice and Bob) is challenging due to photon loss in optical fibers and the probabilistic nature of entanglement generation. Over long distances, the success probability drops exponentially, making direct entanglement impractical.

Quantum repeaters address this issue by dividing the total distance into shorter segments. Through local entanglement generation, purification, and entanglement swapping, these repeaters enable the distribution of entanglement across large distances more efficiently. However, decoherence and operational imperfections can degrade fidelity during swapping, necessitating purification protocols such as BBPSSW to maintain quality.

In this report, we simulate a simplified quantum repeater protocol, incorporating entanglement generation, purification, and swapping across a chain of nodes. The model includes realistic physical parameters like loss and decoherence, illustrating the performance improvements achievable with repeaters.

2. Modeling Assumptions and Implementation

All distances are in kilometers (km) and times in milliseconds (ms).

2.1. Atomic Entanglement Generation

We adopt the Barrett–Kok (BK) protocol. Two end users are linked by an optical fiber with a heralding station at its midpoint. Photons propagate at $c = 2 \times 10^8\ \mathrm{m/s} \approx 0.2\ \mathrm{km/ms}$ so each BK attempt incurs a latency $\tau = 2\frac{L}{2c} = \frac{L}{c}$, where L is the user-to-user separation. The fiber transmissivity is $\eta = e^{-L/L_{\mathrm{att}}},\ L_{\mathrm{att}} = 22.5\ \mathrm{km}$ giving a per-attempt success probability $p_{\mathrm{succ}} = \frac{\eta^2}{2}$. We model entanglement generation as a Bernoulli process, sampling the number of trials until the first success from a geometric distribution; the resulting count multiplied by τ yields the total generation time.

2.2. Network Simulation

To reduce the exponential latency of the BK protocol over long distances, we place N_r quantum repeaters equally spaced between the end users. The network topology is represented by a graph of nodes connected by weighted edges; all quantum-state evolution (unitaries, measurements) is simulated using QuTiP.

Each repeater node executes the following protocol:

1. Initialize two memory qubits, one to entangle with its left neighbor and one with its right.
2. Perform a Bell-state measurement on the two internal qubits.
3. Transmit the measurement outcome (classical bits) to the designated neighbor, who applies the corresponding Pauli correction.

Steps 2–3 take time $o + \tau$, where o is the local-operation latency and τ the classical-communication delay. Disjoint repeaters may perform these operations in parallel.

Entangled links are stored as objects containing the pair of node identifiers and the 4×4 density matrix. To simulate entanglement swapping, we apply the projector $P = I \otimes |\Phi^+\rangle\langle\Phi^+| \otimes I$ to the combined four-qubit state, renormalize, and trace out the two middle qubits. We restrict to the $|\Phi^+\rangle$ outcome (all other Bell-measurement results differ by local Pauli corrections, which we omit explicitly).

To generate end-to-end entanglement, we first use the BK scheme to create entangled links between all $N_r + 1$ adjacent node pairs, collecting them into a list. We then perform *parallel* entanglement-swap rounds: each round groups the current list into disjoint adjacent pairs, swaps all of them simultaneously, and replaces each pair by its swapped link, halving the list length. After $K = \lceil \log_2(N_r + 1) \rceil$ rounds, a single Bell pair remains between Alice and Bob. Since each round requires time $o + \tau$, the total swap time is

$$K\,(o + \tau) \;=\; \lceil \log_2(N_r + 1) \rceil \,\big(o + \tau\big).$$

This completes the idealized end-to-end entanglement simulation.

2.3. Continuous-Time Depolarization Noise Model

In our simulation the only noise source is continuous-time depolarization of each memory qubit. For any entanglement object, the two-qubit density matrix evolves as

$$\rho(t) = e^{-t/T_{\mathrm{depol}}}\,\rho(0) \;+\; \big(1 - e^{-t/T_{\mathrm{depol}}}\big)\,\frac{I_4}{4},$$

where T_{depol} is an adjustable decoherence time and I_4 is the 4×4 identity.

We assume all local unitaries and classical communications are ideal, and that the Barrett–Kok protocol succeeds perfectly up to heralding. After a successful herald, the two memory qubits then depolarize for τ ms while the heralding result is communicated. Each subsequent entanglement-swap round requires $o + \tau$ ms, during which the resulting Bell pair is depolarized for the same interval. No other delays are introduced. This completes our simplified model of continuous-time storage noise.

2.4. Purification Protocol

We employ the BBPSSW protocol to preserve high fidelity in the end-to-end entanglement. Purification is applied at the beginning of each entanglement swap iteration, conditioning on entanglement fidelity below a threshold value. To determine this threshold value, we assume that any two adjacent nodes can prepare an arbitrary number of identical Werner pairs in parallel:

$$\rho = \omega\,|\Phi^+\rangle\langle\Phi^+| \;+\; (1 - \omega)\,\frac{I_4}{4}, \quad \omega \in [0, 1].$$

Each purification round updates the fidelity F and succeeds with probability p_{succ}:

$$F \;\longrightarrow\; \frac{F^2 + \frac{1}{9}(1 - F)^2}{F^2 + \frac{2}{3}\,F(1 - F) + \frac{5}{9}(1 - F)^2}, \tag{1}$$

$$p_{\mathrm{succ}} = F^2 + \tfrac{2}{3}\,F(1 - F) + \tfrac{5}{9}(1 - F)^2. \tag{2}$$

For a lower-bound resource estimate we assume $p_{\mathrm{succ}} = 1$. After purification the state is reset to

$$\rho' = F'\,|\Phi^+\rangle\langle\Phi^+| \;+\; \tfrac{1 - F'}{3}\big(I_4 - |\Phi^+\rangle\langle\Phi^+|\big).$$

To ensure a target fidelity F_{target} between Alice and Bob, we compute the minimum input fidelity required before each swap stage. A single swap on two Werner states of fidelity ω yields fidelity

$$F' = \frac{1 + 3\,\omega^2}{4} = \frac{1 + \frac{(4F-1)^2}{3}}{4}.$$

Requiring $F' > F_{\text{target}}$ gives the threshold

$$F \;>\; \frac{\sqrt{12\,F_{\text{target}} - 3} + 1}{4}.$$

By iterating this inequality backwards through $K = \lceil \log_2 N_{\text{ent}} \rceil$ swap layers, we obtain the minimum fidelity at each layer needed to achieve F_{target} end-to-end. Although this analysis neglects depolarization, it provides a lower bound on the number of purification rounds K required, and we estimate 2^K Werner states cost for this purification process.

2.5. Evaluation Metrics

We evaluate three metrics: (i) entanglement generation time, (ii) end-to-end fidelity, and (iii) the *purification cost*, defined as the average number of Werner pairs consumed per node. To compute this cost, let

$$\{c_0, c_1, \ldots, c_n\}$$

denote the average number of Werner pairs required in iteration k of the entanglement-swap protocol (with c_0 the cost to produce one raw link). Since each purified pair in layer k itself consumes c_{k-1} pairs from layer $k-1$, the total number of raw pairs needed to realize the c_k purified pairs is $\prod_{j=0}^{k} c_j$. Summing over all layers $k = 0, \ldots, n$ gives the total initial Werner-pair cost per node:

$$C_{\text{total}} = \sum_{k=0}^{n} \prod_{j=0}^{k} c_j.$$

We refer to C_{total} as the *final cost* of purification.

3. Experiments and Results

3.1. How do different T_{depol} values affect our results?

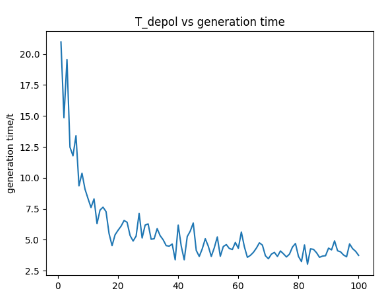

(a) Generation Time

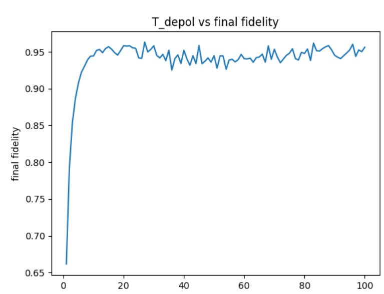

(b) Final Fidelity

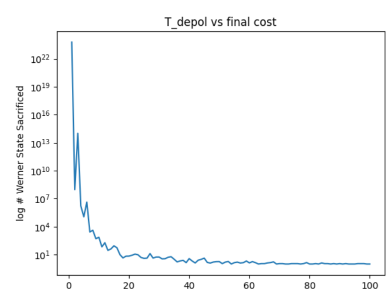

(c) Werner State Cost

Figure 1. Effect of varying T_{depol} on generation time, fidelity, and cost.

The resulting graph from our experiment posted below are using a setting of $L = 200\ km$, representing the distance between Alice and Bob, $num\_nodes = 6$, representing the 6 quantum repeaters between Alice and Bob.

As observed in Figure 2a, the time required to generate entanglement between Alice and Bob decreases as the T_{depol} parameter increases. This is because, when T_{depol} is small, the entangled states decohere more quickly, necessitating more rounds of purification to reach the desired fidelity. These additional purification steps increase the overall generation time.

In contrast, when T_{depol} is large, the effects of decoherence are minimal, reducing the need for purification and resulting in a shorter generation time.

As observed in Figure 2b, the final fidelity increases as the T_{depol} parameter becomes larger. When T_{depol} is small, decoherence causes a significant drop in fidelity, even after purification. Although we apply purification at each entanglement swapping level, the entangled states still decohere during the waiting time and swapping operations. However, with a larger T_{depol}, decoherence becomes negligible, allowing the fidelity to remain high throughout the protocol.

As observed in Figure 2c, when T_{depol} is small, a large number of Werner states are required at each purification level to obtain a single high-fidelity entanglement. Multiplying these numbers across all levels leads to an extremely large total number of Werner states consumed—on the order of 10^{22} in the logarithmic scale. Conversely, when T_{depol} is large, fewer purification steps are needed, significantly reducing the number of Werner states that must be sacrificed.

3.2. What is the maximum amount of noise this protocol can handle and why?

We define the desired fidelity threshold as at least 0.9. Our simulations show that the protocol can successfully generate entanglement with fidelity above 0.9 only when the decoherence time parameter satisfies $T_{\text{depol}} \geq 4$. For values of T_{depol} below 4, the decoherence is too strong, causing excessive noise that the purification steps cannot fully correct. Consequently, the protocol fails to produce high-fidelity entanglement under these conditions.

3.3. What is the minimum number of Werner states we need to sacrifice for purification? Is it still time-efficient?

As observed, when T_{depol} is large, the number of Werner states sacrificed during purification is minimized. The minimum number required in our protocol is $7 \times 4 \times 2 \times 1 = 56$ Werner states. From the first graph, we can see that higher values of T_{depol} correspond to shorter generation times and fewer Werner states needed for purification. Therefore, achieving a larger T_{depol} not only reduces resource consumption but also improves the time efficiency of entanglement generation.

3.4. How does the distance between Alice and Bob influence the entanglement generation?

To explore the effect of distance on entanglement generation, we set $T_{\text{depol}} = 10$ and varied the number of nodes from 4 to 40 for three different distances: $L = 200$, 500, and 1000.

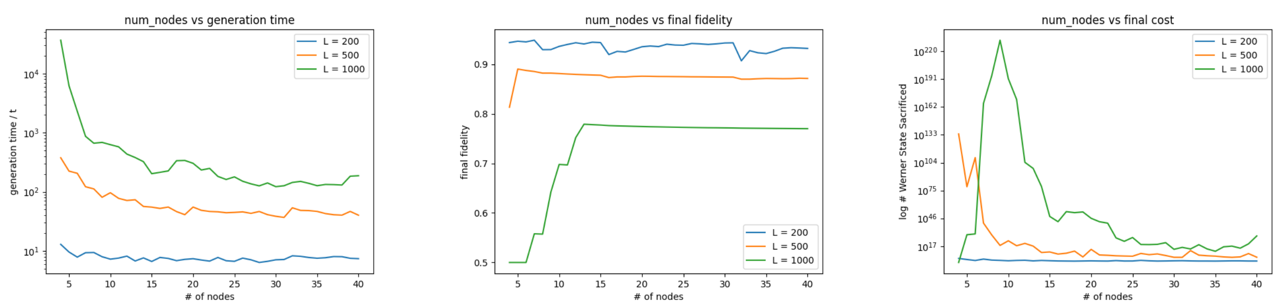

(a) Generation Time (b) Final Fidelity (c) Werner State Cost

Figure 2. Effect of L on generation time, fidelity, and cost.

As shown in the figures, increasing the distance L between Alice and Bob results in longer generation times. This is because greater distances lead to increased decoherence and loss, requiring more rounds of purification to achieve the target fidelity. Additionally, the final fidelity decreases with larger L, since decoherence has a stronger impact over longer transmission times—even when purification is applied repeatedly. Finally, the number of Werner states sacrificed also increases with distance, as more resources are needed to mitigate the effects of decoherence and maintain acceptable fidelity levels.

3.5. How does the number of quantum repeaters affect entanglement generation?

From the previous graphs, we observe that for each value of L, increasing the number of quantum repeaters consistently improves performance. As the number of intermediate nodes increases, the required generation time decreases, and fewer

Werner states are sacrificed during purification.

It is important to note that the optimal number of repeaters for achieving the highest final fidelity depends on the total distance L. For example, at $L = 200$, the maximum fidelity is achieved with $n = 6$ nodes. For $L = 500$, the peak fidelity occurs at $n = 8$, and for $L = 1000$, it occurs around $n = 13$.

In general, a moderate number of quantum repeaters is sufficient to achieve high final fidelity. However, if the goal is to minimize generation time and resource consumption, it is beneficial to deploy more repeaters between Alice and Bob.

4. Conclusion

In this project, we simulated a quantum network architecture leveraging quantum repeaters to efficiently generate high-fidelity entanglement between two distant parties—Alice and Bob—under realistic physical constraints such as decoherence and limited entanglement success rates. By modeling the Barrett-Kok (BK) protocol for entanglement generation, incorporating continuous-time depolarization as the primary noise model, and applying the BBPSSW purification protocol, we were able to assess the impact of decoherence on fidelity, time, and resource consumption.

Our experiments demonstrate that the entanglement generation time and purification cost grow rapidly with increased noise, while high decoherence (i.e., low T_{depol}) severely limits the final fidelity. Specifically, we observed that maintaining $T_{\text{depol}} \geq 4$ ms is necessary to achieve end-to-end fidelity above 0.9. Moreover, we quantified the number of Werner states sacrificed in purification, highlighting the trade-off between fidelity and resource efficiency.

This simulation confirms the critical importance of purification and the strategic placement of quantum repeaters in real-world quantum communication systems. While simplifications were made (e.g., perfect operations and heralding), our model captures key insights into optimizing quantum network performance and serves as a foundation for future extensions involving realistic hardware constraints. However, our results also verified that the purification scheme requires Werner states exponentially increasing with respect to distance, and this will lead us to explore alternative entanglement distribution schemes, and error correction techniques.